Available online at www.sciencedirect.com
SCIENCE DIRECT®
Journal of Solid State Chemistry 177 (2004) 3339–3345
JOURNAL OF SOLID STATE CHEMISTRY
http://elsevier.com/locate/jssc

Metamagnetism in $DyBaCo_2O_{5+x}$, $x \approx 0.5$

H.D. Zhou* and J.B. Goodenough

Texas Materials Institute, ETC 9.102, 1 University Station, C2201, University of Texas at Austin, Austin, TX 78712-1063, USA

Received 14 April 2004; received in revised form 20 May 2004; accepted 23 May 2004

Available online 20 July 2004

Abstract

The temperature dependence of the paramagnetic susceptibility $\chi_m(T)$ taken in 2500 Oe, the resistivity $\rho(T)$, and the thermoelectric power $\alpha(T)$ of $DyBaCo_2O_{5+x}$, which has Ba and Dy ordered into alternate (001) planes of an oxygen-deficient perovskite, have revealed a phase segregation in the compositional range $0.3 \leqslant x < 0.5$. Orthorhombic $DyBaCo_2O_{5.51}$ has, in addition, oxygen vacancies ordered into alternate rows of the $DyO_{0.51}$ (001) planes; a cold-pressed polycrystalline sample exhibits a first-order insulator–metal transition at $T_{IM} = 320$ K, a Curie temperature $T_C = 300$ K, and a broadened metamagnetic transition temperature $T_M \approx 265$ K in 2500 Oe. A ferromagnetic $M-H$ hysteresis curve fails to saturate at 5 T, and a minority ferromagnetic phase below T_M has a volume fraction that decreases with decreasing temperature, vanishing below 50 K. Oxygen vacancies in the $DyBaCo_2O_{5.5}$ phase suppress the metallic state; interstitial oxygen does not. A thermoelectric power $\alpha(T) > 0$ of $DyBaCo_2O_{5.51}$ changing continuously across T_{IM} is interpreted to manifest a metallic minority phase crossing a percolation threshold; $\alpha(T)$ also provides evidence for a progressive excitation of higher-spin Co(III) with increasing temperature from below 50 K to above T_{IM}. A previous model of the $RBaCo_2O_{5.5}$ phase is extended to account for the Ising spin configuration below T_C, the magnetic order in the presence of higher-spin octahedral-site Co(III), and the $\alpha(T)$ data.

Keywords: Cobaltites; Spin-state transitions; Orbital ordering; Oxygen-deficient perovskites

1. Introduction

The $RBaCo_2O_{5.5}$ family has the larger Ba^{2+} and smaller rare-earth R^{3+} ions ordered into alternate (001) planes of a tetragonal perovskite structure; the oxygen vacancies are confined to the $RO_{0.5}$ (001) planes. With a primitive cubic perovskite lattice parameter a_p, the structure is tetragonal ($1a_p \times 1a_p \times 2a_p$) where the oxygen vacancies are disordered in the $RO_{0.5}$ (001) planes; it is orthorhombic *Pmmm* ($2a_p \times 1a_p \times 2a_p$) where the oxygen vacancies order into alternate [010] rows within the $RO_{0.5}$ (001) planes [1]. This ordering creates alternating [010] rows of square-pyramidal and octahedral Co(III) sites, Fig. 1. The square-pyramidal sites form two-leg ladders aligned parallel to the *b*-axis; they are coupled along the *a*-axis across (010) planes of corner-shared octahedra and along the *c*-axis across oxygen vacancies.

The orthorhombic phase is metallic above a first-order insulator–metal transition at a temperature T_{IM} that increases with the size of the rare-earth ion over the range $310\ K \leqslant T_{IM} \leqslant 360\ K$ for $R = Dy, \ldots, Eu$ [2–4]. In a small temperature interval $T_M \leqslant T \leqslant T_C$, where $T_C < T_{IM}$, the orthorhombic phases are ferromagnetic; but below a metamagnetic transition temperature T_M, they became antiferromagnetic in zero applied magnetic field. Below T_M, the ferromagnetic phase is restored above a critical magnetic field strength $H_c(T)$ that increases with decreasing temperature. Moreover, metallic behavior above a T_{IM} is peculiar to the oxygen stoichiometry $RBaCo_2O_{5.5-\delta}$ with $\delta \geqslant 0$; the high-temperature metallic phase can tolerate a little excess oxygen, but additional oxygen vacancies suppress the transition at T_{IM} to a metallic state.

It has been recognized that the key to understanding these phenomena may be the variation with temperature of the spin state of the Co(III) ions. In the $RCoO_3$ perovskites, the octahedral-site Co(III) ions are in their low-spin (LS) state t^6e^0 at low temperatures, but with

*Corresponding author. Fax: +1-512-471-7681.
E-mail address: hdzhou@physics.utexas.edu (H.D. Zhou).

0022-4596/$ - see front matter © 2004 Elsevier Inc. All rights reserved.
doi:10.1016/j.jssc.2004.05.047

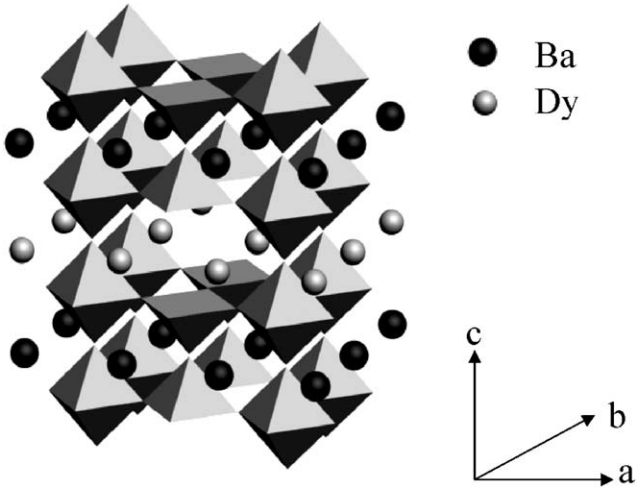

Fig. 1. Schematic crystal structure of $DyBaCo_2O_{5.5}$.

increasing temperature they convert to the intermediate-spin (IS) state t^5e^1 and/or to the high-spin (HS) state t^4e^2 as a result of the thermal expansion of the site and the higher entropy of the higher spin states. Moreover, a smooth insulator-metal transition near 600 K in $LaCoO_3$ reflects the growth of an itinerant-electron phase to beyond percolation in a localized-electron matrix; the itinerant electrons occupy a narrow σ^* band of e-orbital parentage in a phase having a higher concentration of HS Co(III) ions. These observations have suggested that the insulator–metal transition at T_{IM} may be associated with a transition from the LS to the HS state at the octahedral-site Co(III) in $RBaCo_2O_{5.5}$ compounds, and Frontera et al. [5] have reported an anomalous volume expansion on increasing the temperature across T_{IM} in $GdBaCo_2O_{5.5}$. On the other hand, the five-fold oxygen coordination at the square-pyramidal Co(III) sites can be predicted to stabilize the IS state at all temperatures, and a study by Taskin et al. [6a] of the magnetic susceptibility of a detwinned $GdBaCo_2O_{5.5}$ single crystal has provided clear evidence for the ferromagnetic moment coming from an IS Co(III) on the square-pyramidal sites having a spin $S=1$ pinned along the b-axis. They argued convincingly that the spins within a square-pyramidal two-leg ladder are strongly coupled ferromagnetically to give a $T_C \approx 300$ K and that the metamagnetic transition is associated with a weaker interladder coupling. They also pointed out that a changing population below T_{IM} of higher-spin octahedral-site Co(III) could be responsible for a change in the sign of the a-axis coupling between ferromagnetic $b-c$ planes of square-pyramidal IS Co(III) across $b-c$ planes of octahedral-site Co(III).

In this paper, we report the temperature dependences of the thermoelectric power $\alpha(T)$, the resistivity $\rho(T)$, and the magnetic susceptibility $\chi_m(T)$ of cold-pressed, polycrystalline $DyBaCo_2O_{5+x}$, $0.005 \leqslant x \leqslant 0.51$, samples. We extend the model of Taskin et al. [6a] for $x=0.5$ by considering the origin of the Ising-like behavior of the spins of the IS Co(III) on the square-pyramidal sites and the magnetic coupling between any HS Co(III) ions within the octahedral-site b–c planes. The influence of added oxygen vacancies on the transport and magnetic properties of $DyBaCo_2O_{5.5}$ is also discussed.

2. Experimental

Polycrystalline samples of $DyBaCo_2O_{5+x}$ ($0.005 \leqslant x \leqslant 0.51$) were prepared by standard solid-state reaction. Stoichiometric mixtures of Dy_2O_3, $BaCO_3$, and Co_3O_4 were ground and calcined in air at 1150°C for 24 h. The product was then reground, pelletized, and sintered at 1150°C for another 24 h in air. The stoichiometry of the as-prepared sample was $DyBaCo_2O_{5.21(2)}$ as determined by thermogravimetric analysis (TGA) under a flowing mixture of 5% H_2Ar at 1000°C. The as-prepared sample was also single phase to powder X-ray diffraction. The TGA curve of Fig. 2 taken in oxygen provided a guide as to how to obtain samples with different oxygen content. The as-prepared sample was then cold-pressed and annealed in the TGA apparatus at different temperatures in either pure oxygen or argon to adjust the oxygen content; weight change was used to calculate the oxygen stoichiometries of the end products. As prepared samples were annealed in pure oxygen for 10 h at 230°C, 210°C and 180°C leading to x values 0.51(1), 0.46(2), and 0.31(1), respectively; the values $x=$ 0.115(3) and 0.005(3) were obtained after annealing in argon for 8 h at 410°C and for 30 min at 1000°C, respectively.

A room temperature powder X-ray diffraction pattern for $DyBaCo_2O_{5.51}$ was also recorded with a Philips 1729 diffractometer equipped with a pyrolytic-graphite monochromator and Cu$K\alpha$ radiation; Si was

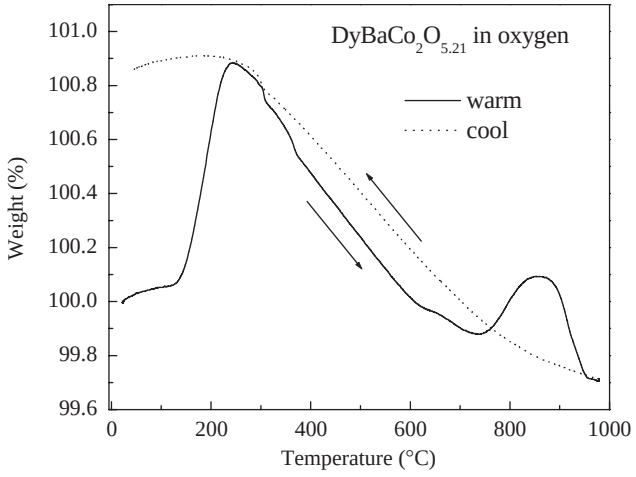

Fig. 2. Thermogravimetric (TGA) curve of $DyBaCo_2O_{5.21}$ taken in an oxygen flow at a heating and cooling rate of 1°C/min; solid line is the heating process and dotted line is the cooling process.

the internal standard. Data were collected in steps of 0.020° over the range $20° \leqslant 2\theta \leqslant 80°$ with a count time of 15 s per step. Peak profiles were fitted with the program JADE. $DyBaCo_2O_{5.51}$ has the orthorhombic *Pmmm* structure with lattice parameters $a = 7.725(1)$Å, $b = 3.904(2)$Å, and $c = 7.509(3)$Å, which corresponds to the $2a_p \times 1a_p \times 2a_p$ superstructure reported by Akahoshi and Ueda [1] for $YBaCo_2O_{5.5}$.

Magnetic-susceptibility measurements were made with a Quantum Design DC SQUID magnetometer after cooling in zero field (ZFC) or after cooling in a measuring field (FC) of 2500 Oe. *M–H* hysteresis loops of magnetization *M* versus applied magnetic field *H* were measured over the range $-5\,T \leqslant H \leqslant 5\,T$ at 265 and 180 K.

The thermoelectric power $\alpha(T)$ was obtained with a laboratory-built apparatus as described elsewhere [7]. The resistivity $\rho(T)$ was measured by a four-probe technique.

3. Results

Fig. 3 shows the temperature dependences of the molar magnetic susceptibility $\chi_m(T)$ and its inverse $\chi_m^{-1}(T)$, the resistivity $\rho(T)$, and the thermoelectric power $\alpha(T)$ for orthorhombic (*Pmmm*) $DyBaCo_2O_{5.51}$. Clearly evident are an insulator–metal transition at $T_{IM} \approx 320$ K where the resistivity changes from 10^{-1} to $10^{-3}\,\Omega$cm, a ferromagnetic Curie temperature $T_C \approx 300$ K, and a metamagnetic transition temperature $T_M \approx 265$ K in 2500 Oe. Lowering the applied field strength sharpens the transition at T_M. We were not able to obtain reliable values for $\alpha(T)$ below 120 K; in the interval $120\,K < T < 180\,K$, an Arrhenius plot of $\alpha(T)$ gave a trapping energy for mobile Co(IV) polarons of $\Delta H_t/2 = 14$ meV and an Arrhenius plot of $\rho(T)$ over the same temperature interval gave an activation energy $E_a = \Delta H_m + (\Delta H_t/2) = 80$ meV corresponding to a motional enthalpy $\Delta H_m = 66$ meV for the Co(IV) ions.

Fig. 4 shows $M-H$ hysteresis loops taken at $T = 265\,K \approx T_M$ and $T = 180\,K < T_M$ for $DyBaCo_2O_{5.51}$. Lack of saturation at 50 KOe in our polycrystalline sample is consistent with the Ising-like behavior of the spins reported by Taskin et al. [6a]. Although the remanence is strongly reduced at $T = 180$ K from that at 265 K, nevertheless a residual ferromagnetic component is retained as is also evident in the divergence of the ZFC versus FC $\chi_m(T)$ curves of Fig. 3.

Fig. 5 shows that as oxygen is removed from $DyBaCo_2O_{5.5}$, the volume fraction of the ferromagnetic phase decreases, vanishing by $DyBaCo_2O_{5.21}$. Moreover, the $\rho(T)$ curve for $DyBaCo_2O_{5.46}$, not shown, exhibits no anomaly at a T_{IM}; the compound remains polaronic at higher temperatures. The insulator–metal

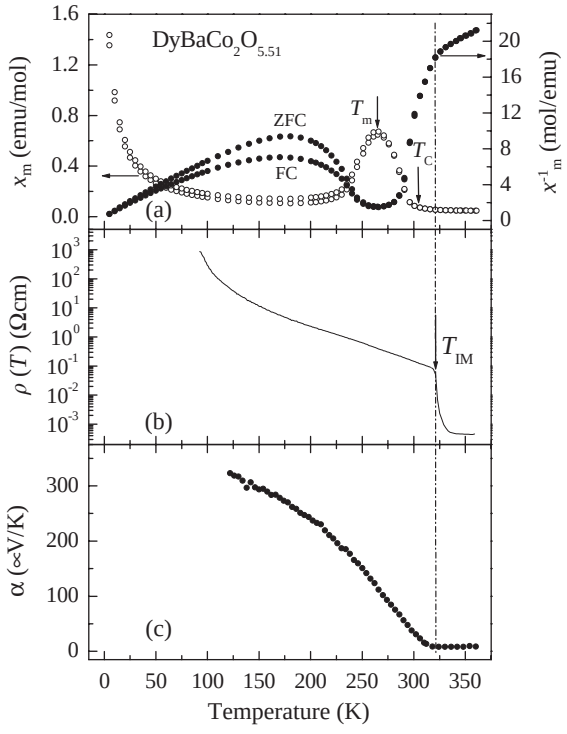

Fig. 3. (a) Molar magnetic susceptibility $\chi_m(T)$ and its inverse $\chi_m^{-1}(T)$, (b) resistivity $\rho(T)$, and (c) thermoelectric power $\alpha(T)$ of $DyBaCo_2O_{5.51}$.

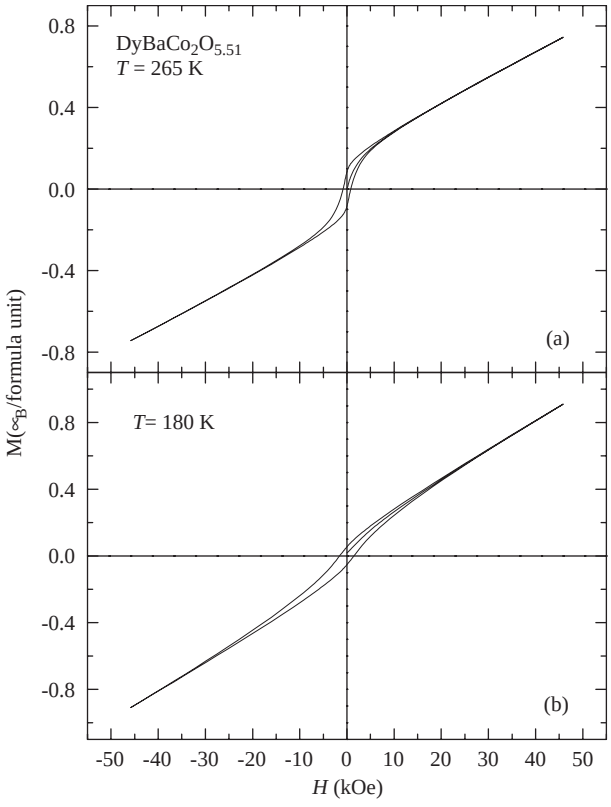

Fig. 4. Field dependences of magnetization of $DyBaCo_2O_{5.51}$ measured at (a) 265 K and (b) 180 K.

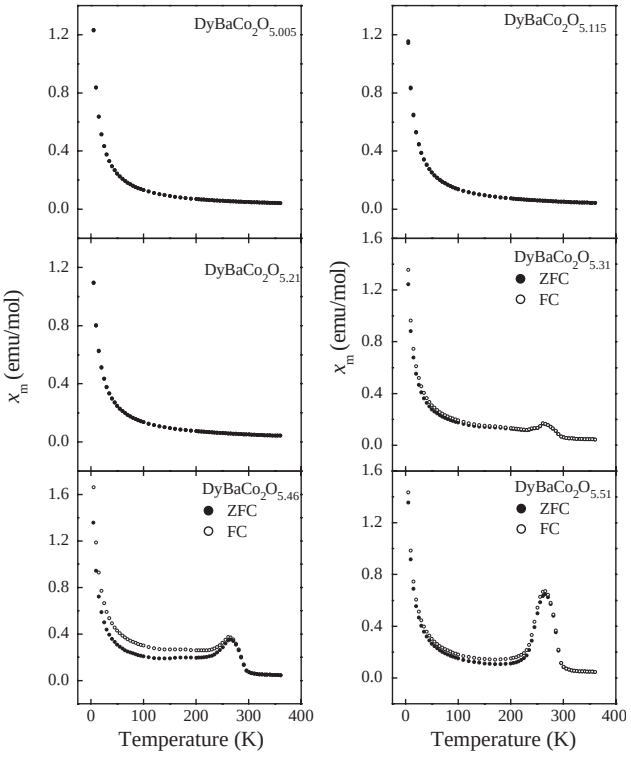

Fig. 5. Molar magnetic susceptibility $\chi_m(T)$ for $DyBaCo_2O_{5+x}$ ($0.005 \leqslant x \leqslant 0.51$), for $x = 0.005$, 0.115 and 0.21 ZFC and FC curves overlap.

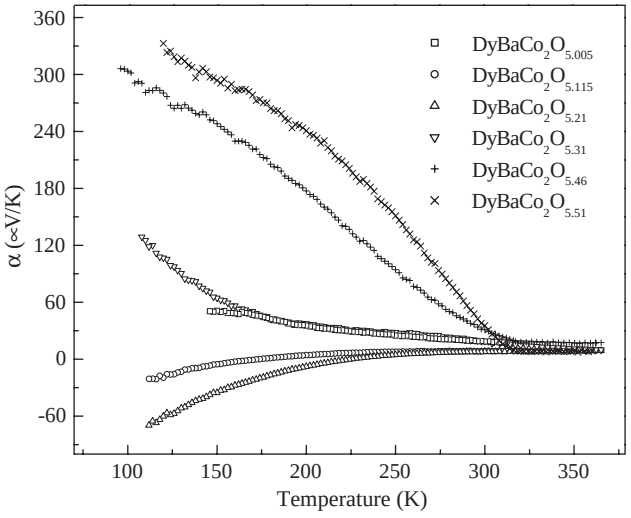

Fig. 6. Thermoelectric power $\alpha(T)$ for $DyBaCo_2O_{5+x}$ ($0.005 \leqslant x \leqslant 0.51$).

transition is completely suppressed with only 0.04 oxygen vacancies per formula unit in the octahedral-site b–c plane even though $\alpha(T)$ shows a sharper increase on cooling below T_C in Fig. 6. This figure also shows that low-temperature $\alpha(T)$ becomes negative for $x = 0.21$, returning to a positive value at $x = 0.005$ in $DyBaCo_2O_{5+x}$, Taskin et al. [6b] also observed a change in the sign of $\alpha(T)$ in $GdBaCo_2O_{5+x}$.

4. Discussion

$DyBaCo_2O_{5.5}$ is a distinguishable phase that can accept some excess oxygen; it is a p-type conductor in both the polaronic and metallic states. Compositions $DyBaCo_2O_{5+x}$ with $0.3 \leqslant x < 0.5$ segregate into two phases, one corresponding to p-type $x = 0.5$ and the other to a phase that is n-type with $0.21 < x < 0.31$. Both of these segregated phases are semiconductive at all temperatures where they coexist. In $DyBaCo_2O_{5.5+\delta}$, the mobile holes are progressively trapped out as the temperature decreases below T_{IM}. The square-pyramidal site Co(III) ions have been shown [6a] to be in the IS state at all temperatures and the octahedral-site Co(III) to be in their low-spin state at low temperatures, which we take to be $T < 180$ K. At temperatures $T < 180$ K, the holes are small-polaron Co(IV) ions that are progressively trapped out by shallow trapping centers; these traps are probably octahedral sites neighboring an interstitial oxygen that introduced the Co(IV) ions. The origin of an increase in $E_a = \Delta H_m + (\Delta H_t/2)$ below 105 K is not identified; it could represent a condensation of the holes into ordered clusters. The paramagnetic susceptibility data of Frontera et al. [5] for $T > T_{IM}$ are consistent with HS Co(III) in the octahedral sites and IS Co(III) in the square-pyramidal sites in the metallic phase. At $T > T_{IM}$, the spin degeneracy of the electrons of e-orbital parentage is removed by the intraatomic exchange with the localized spins of the π-bonding t electrons, and spin-disorder scattering can account for poor-metal behavior with an $\alpha > 0$ if the octahedral-site Co(III) are in their HS state.

The smooth non-Arrhenius increases in $\alpha(T)$ and $\rho(T)$ on cooling $DyBaCo_2O_{5.51}$ through the interval $180\text{ K} < T < T_{IM}$ must, it follows, be associated with the transition from LS to HS octahedral-site Co(III) on the approach to T_{IM}. The fact that a positive $\alpha(T)$ is retained as the population of electrons in the e-orbitals decreases to zero appears to require the coexistence of two phases, one containing mostly HS Co(III) and the other mostly LS Co(III) on the octahedral sites. Either the metallic, HS–Co(III) phase becomes non-percolative below T_{IM} or the conductivity of the HS Co(III) phase is made polaronic by the perturbation of the periodic potential by the second phase; the latter phenomenon is observed in $DyBaCo_2O_{5.46}$ where the metallic phase above T_{IM} is transformed to a polaronic phase with $\alpha(T) > 0$ by the coexistence of a second phase. As the volume fraction of the HS Co(III) phase decreases, the mobile holes would be transferred progressively into low-spin Co(IV) small polarons in the LS-Co(III) phase. The coexistence of two phases is consistent with the first-order character of the transition at T_{IM}. This HS–LS phase segregation is to be distinguished from the phase separation occurring in the compositional range $0.31 \leqslant x < 0.5$.

Discussion of the magnetic data begins with the observation of Taskin et al. [6a] that the spins of the IS Co(III) on the square-pyramidal sites are pinned to the *b*-axis to give an Ising magnetic lattice and with their observation that the square-pyramidal sites form two-leg ladders within which the spins are strongly coupled ferromagnetically to give a $T_C \approx 300$ K. They also pointed out that coupling between ladders across a Co(III) octahedral-site $b-c$ plane could change sign as the population of octahedral-site LS Co(III) increased with decreasing temperature. They retained a ferromagnetic coupling between ladders along the *c*-axis across an oxygen vacancy. In addition, they showed that an *e*-orbital ordering on the IS Co(III) ions like that shown in Fig. 7 could account for the ferromagnetic coupling with the Goodenough–Kanamori rules for the sign of the spin–spin exchange interactions. An *e*-orbital ordering that alternates occupancy of (x^2-y^2) and $(3z^2-r^2)$ orbitals on traversing a leg of a two-leg ladder with out-of-phase ordering on the second leg requires asymmetric Co···O–Co bonds in both the rungs and legs of the ladder, and these displacements were not detected by the diffraction experiments of either Frontera et al. [5] or Moritomo et al. [8]. However, a lack of long-range order or a vibronic coupling with quasi-static long-range order would make it difficult to detect atomic displacements within the ladders. It is also possible to achieve ferromagnetic order within the ladders and between ladders along the *c*-axis across an oxygen vacancy by an *e*-orbital ordering that alternates occupancy of $(3x^2-r^2)$ and $(3z^2-r^2)$ orbitals on traversing a leg of a ladder with out-of-phase orbital ordering

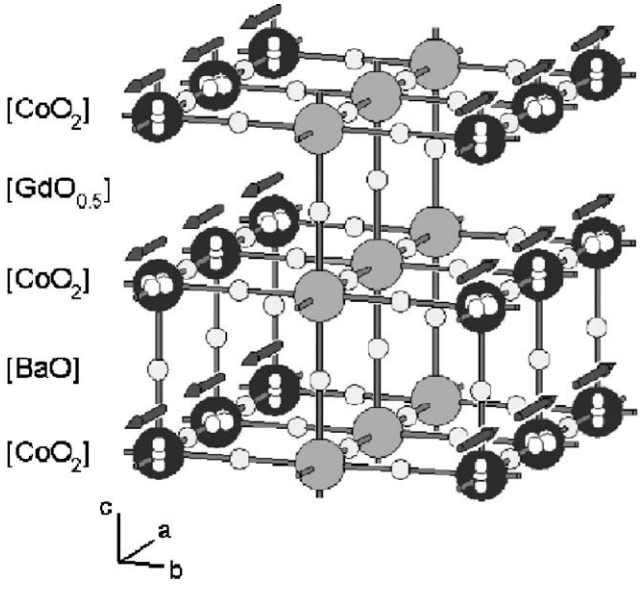

Fig. 7. Schematic *e*-orbital ordering of $GdBaCo_2O_{5.5}$ suggested by Taskin et al. [6a].

on the other leg. Since the *e*-orbital ordering responsible for the ferromagnetic interactions within the ladders is ambiguous, we begin with a consideration of the origin of the pinning of the Co(III) spins of the two-leg ladders along the axis of the legs.

In an octahedral site, an IS Co(III): t^5e^1 configuration has a three-fold *t*-orbital degeneracy as well as a two-fold *e*-orbital degeneracy. In a square-pyramidal site, these degeneracies are removed, but the cation displacement toward the apical oxygen determines how the orbital degeneracies are removed. In addition, atomic displacements within the CoO_2 (001) sheets influence how the *t*-orbital degeneracy is removed. The observation of an Ising spin lattice within the ladders signals that there is an unquenched orbital angular momentum that is oriented along the ladder legs and that it is pinned by a strong elastic force. This observation can only mean that the *t*-orbital hole of an IS Co(III) occupies a $(yz \pm izx)$ orbital.

This conclusion would be compatible with a contraction of the *b*-axis on cooling through T_{IM} as reported by Moritomo et al. [8], but Frontera et al. [5] as well as Akahoshi and Ueda [9] have reported that the *b*-axis expands on cooling through T_{IM}. A transition from HS to LS on the octahedral-site Co(III) should contract the lattice parameters, and indeed two axes and the volume contract on cooling through T_{IM}; but one axis expands, and it appears to be the ladder axis *b*. One of us [10] has argued from the virial theorem that the equilibrium (M–O) bond length associated with localized *d* electrons is longer than the equilibrium bond length where the *d* electrons become itinerant, and this prediction has been extensively validated by experiment. Therefore, an elongation of the ladder axis on cooling through T_{IM} may reflect the transition from itinerant to localized behavior of the *e* electrons where no spin-state transition occurs. We are thus led to conclude that the *t*-orbital ordering is present above as well as below T_{IM} and that the *t*-orbital hole occupies a $(yz \pm izx)$ orbital below T_{IM} at the sites where the $(3z^2-r^2)$ orbital is occupied; at the other IS Co(III) sites of a ladder leg, the Co–O_a bonds should be lengthened so as to introduce stabilization of a hybrid $(3x^2-r^2)$ and (x^2-y^2) orbital that lifts the *t*-orbital degeneracy without quenching significantly the orbital angular momentum oriented along the *b*-axis. The ferromagnetic exchange with the pinned spins would then keep all the spins pinned to the *b*-axis. Note that this model hybridizes the two possible solutions discussed above for the *e*-orbital ordering. The magnetic data thus suggest the individual (Co–O) bond lengths are more complex than those obtained in previous structural studies.

A significant HS population on the octahedral-site Co(III) at T_C, which is indicated by the $\alpha(T)$ data, would strongly couple the ladder legs ferromagnetically across the octahedral-site Co(III) $b-c$ planes since

antiferromagnetic coupling within the octahedral-site planes would match parallel spins with $(3z^2-r^2)$ spins in the ladders and antiparallel spins with $(3x^2-r^2)$, (x^2-y^2) spins in the ladders. This magnetic order would give antiferromagnetic coupling with octahedral-site b–c plane and a ferromagnetic moment from the square-pyramidal sites equal to the ferromagnetic moment reported by Taskin et al. [6a]. As the population of HS Co(III) in the octahedral sites decreases, the model calls for a segregation within octahedral-site Co(III) planes of islands of LS Co(III) that grow with decreasing temperature. Across a LS Co(III), the $(3x^2-r^2)$, (x^2-y^2) spins of neighboring ladders interact antiferromagnetically. Above a critical fraction of LS Co(III), the a-axis coupling between ladders changes sign to give the metamagnetic behavior below T_M. However, the two-phase character of the LS–HS transition is manifest in the retention of a ferromagnetic minority phase within the metamagnetic matrix to quite low temperature as is manifest by the divergence of the FC and ZFC $\chi_m(T)$ curves in Fig. 3.

Reduction of the volume fraction of the ferromagnetic phase below T_C in $DyBaCo_2O_{5.46}$, Fig. 5, is indicative of a two-phase character in the compositions $0.3 \leqslant x < 0.5$ of $DyBaCo_2O_{5+x}$; but this observation begs the question of why the metallic phase above a T_{IM} is suppressed in the $DyBaCo_2O_{5.5}$ phase within this composition. Establishing a σ^* band of itinerant-electron states of e-orbital parentage in an octahedral-site Co(III) array depends not only on a critical population of HS Co(III) ions, but also on an unperturbed periodic potential and an e–O–e overlap integral that exceeds a critical value. Since the metallic phase is at the threshold of its formation, it would not take a large perturbation to suppress it. The limiting composition of the $DyBa_2Co_2O_{5.5}$ phase can be expected to contain some oxygen vacancies. Every oxygen vacancy introduces two HS Co(III) ions having localized t^5e^2 configurations; both species would perturb the periodic potential. The introduction of only a small concentration of oxygen vacancies into the $DyBaCo_2O_{5.5}$ phase appears to be sufficient to suppress the transition to the metallic phase.

5. Conclusions

Orthorhombic $DyBaCo_2O_{5.5}$ contains an ordering of Ba and Dy ions into alternate (001) planes of the perovskite structure and an ordering of oxygen vacancies into alternate [010] rows in the $DyO_{0.5}$ planes. This ordering creates two-leg ladders parallel to the b-axis of IS Co(III) ions in square-pyramidal sites; the ladders of a b–c plane are separated by an oxygen vacancy, but the ladder spins of the b–c planes remain ferromagnetically coupled below T_C and pinned to the b-axis. The ladder spins of neighboring b–c planes are coupled across octahedral-site Co(III) ions, and the sign of this coupling changes from antiferromagnetic to ferromagnetic at T_M as the population of higher-spin Co(III) on the octahedral sites increases with temperature. However, a ferromagnetic volume fraction persists below T_M; this fraction decreases with decreasing temperature, disappearing below 50 K. Moreover, with spins pinned to the b-axis and $T_M = T_M(H)$, a $T_M(2500\,Oe) \approx 265\,K$ is broadened.

A postulated model of orbital ordering that can account for the magnetic order and the pinning of the spins along the b-axis provides a net magnetization in the ferromagnetic planes that is due to only the spins in the square-pyramidal sites; the spins of the higher-spin octahedral-site Co(III) would have a net antiferromagnetic order. The population of higher-spin Co(III) on the octahedral sites increases progressively with temperature to T_{IM} where a small step increase occurs. However, the thermoelectric power remains positive and changes continuously across T_{IM}, which suggest the coexistence of a metallic phase and a polaronic phase across T_{IM} with the volume fraction of the metallic phase increasing discontinuously to beyond a percolation threshold at T_{IM}.

The introduction of oxygen vacancies into the b–c planes of octahedral-site Co(III) suppresses the insulator–metal transition, but not T_C and T_M; and a progressive decrease with x in the volume fraction of the ferromagnetic phase in the interval $T_M < T < T_C$ found in the compositional range $0.2 < x < 0.5$ of $DyBaCo_2O_{5+x}$ signals separation into two polaronic phases of different x. At the phase limit $DyBaCo_2O_{5.5-\delta}$ with $0 < \delta < 0.04$, the metallic phase of $DyBaCo_2O_{5.5}$ is completely suppressed.

Acknowledgments

The authors thank the National Science Foundation and the Robert A. Welch Foundation of Houston, Texas, for financial support.

References

[1] D. Akahoshi, Y. Ueda, J. Phys. Soc. Japan 68 (1999) 736.
[2] I.O. Troyanchuk, N.V. Kasper, D.D. Khalyavin, H. Szymczak, R. Szymczak, M. Baran, Phys. Rev. Lett. 80 (1998) 3380; I.O. Troyanchuk, N.V. Kasper, D.D. Khalyavin, H. Szymczak, R. Szymczak, M. Baran, Phys. Rev. B 58 (1998) 2418.
[3] Y. Moritomo, M. Takeo, X.J. Liu, T. Akimoto, A. Nakamura, Phys. Rev. B 58 (1998) R13334.
[4] A. Maignan, C. Martin, D. Pelloquin, N. Nguyen, B. Raveau, J. Solid State Chem. 142 (1999) 247.
[5] C. Frontera, J.L. Garcìa-Muñoz, A. Llobet, M.A.G. Aranda, Phys. Rev. B 65 (2002) 180405.
[6] (a) A.A. Taskin, A.N. Lavrov, Y. Ando, Phys. Rev. Lett. 90 (2003) 227201;

(b) A.A. Taskin, A.N. Lavrov, Y. Ando, Proceedings, Twenty-second International Conference on Thermoelectrics, P196–200, IEEE Publisher, New York, 2003.
[7] J.B. Goodenough, J.-S. Zhou, J. Chen, Phys. Rev. B 47 (1993) 5275.
[8] Y. Moritomo, T. Akimoto, M. Takeo, A. Machida, E. Nishibori, M. Takata, M. Sakata, K. Ohoyama, A. Nakamura, Phys. Rev. B 61 (2000) R13325.
[9] D. Akahoshi, Y. Ueda, J. Solid State Chem. 156 (2001) 355.
[10] J.B. Goodenough, Struct. Bonding 98 (2001) 1.